

Analysis of onset of buoyancy-driven convection in a fluid layer saturated in anisotropic porous media by the relaxed energy method

Min Chan Kim[†]

Department of Chemical Engineering, Jeju National University, Jeju 690-756, Korea

(Received 7 January 2013 • accepted 3 March 2013)

Abstract—A theoretical analysis of buoyancy-driven instability under transient basic fields is conducted in an initially quiescent, fluid-saturated, horizontal porous layer. Darcy's law is used to explain characteristics of fluid motion, and the anisotropy of permeability is considered. Under the Boussinesq approximation, the energy stability equations are derived following the energy formulation. The stability equations are analyzed numerically under the relaxed energy stability concept. For the various anisotropic ratios, the critical times are predicted as a function of the Darcy-Rayleigh number, and the critical Darcy-Rayleigh number is also obtained. The present predictions are compared with existing theoretical ones.

Key words: Buoyancy-driven Convection, Anisotropic Porous Medium, Energy Method

INTRODUCTION

Buoyancy-driven phenomena in porous media play an important role in a wide variety of engineering applications, such as geothermal reservoirs, agricultural product storage system, packed-bed catalytic reactors and pollutant transport under the ground. One of the attractive convection phenomena in porous media is the naturally enhanced carbon dioxide (CO_2) dissolution into the saline water confined within the geologically stable formations [1-10]. In this particular case the heavier CO_2 saturated water will flow downward and will be replaced by water with lesser CO_2 content. Although the density increase of CO_2 is only around 1% at subsurface conditions, on long time scales this can lead to a convective mixing process, which significantly accelerates the dissolution of CO_2 , and thus improves the containment.

The onset of buoyancy-driven convective instabilities in porous media was first analyzed by Horton and Rogers [11] and independently by Lapwood [12]. They examined thermally driven convection and used the methods developed for convection in a homogeneous fluid under the assumption of the linear and time-independent temperature profile. However, for the case of transient nonlinear temperature or concentration field, the related instability has been analyzed by using the frozen-time model [13], the energy method [1,4,5,13], and the linear amplification theory [1,4,5,13]. All of these methods have a parallel history of application in the Rayleigh-Bénard convection. The first model is based on linear theory and yields the critical time as a parameter based on the quasi-static approximation. In the energy method, the generalized energy functional is derived and the parameter range at which finite disturbances will decay exponentially. The last method is an initial value model that requires the initial conditions at the time $t=0$ and the criterion to define manifest convection. Riaz et al. [3] analyzed the onset of convection in porous media under the time-dependent concentration field in self-

similar coordinate. Their basic idea is quite similar to the propagation theory [14]. Recently, for the isotropic porous media, Selim and Rees [15], Hassanzadeh et al. [16] and Kim and Choi [17] reconsidered the present transient problem by employing linear stability analysis, direct numerical simulation and modified energy method, respectively. Under the linear stability theory Rapaka et al. [6] and Hidalgo et al. [7] introduced the nonmodal stability concept into the present problem. For isotropic and anisotropic media, they found the most unstable infinitesimal disturbances for a specified condition. Further historical review can be found in Nield and Bejan [18].

In the present study the onset of buoyancy-driven convection in anisotropic porous media is investigated by the relaxed energy method. Even though Ennis-King et al. [1], Hassanzadeh et al. [4], Xu et al. [5], and Hong and Kim [19] considered this problem by employing the energy method, their results are slightly different from each other. In the present work, their results are compared and extended to a larger time region. Therefore, the present work may be the complement and extension of the previous work [1,4,5,19].

THEORETICAL ANALYSIS

1. Governing Equations

The system considered here is an initially quiescent, fluid-saturated, horizontal porous layer of depth d , as shown in Fig. 1. Initially, the fluid layer contains no solute, i.e., $C=0$ at $t=0$. For time $t \geq 0$, the gas starts to dissolve into the fluid layer through the upper free boundary which is assumed to be maintained at uniform con-

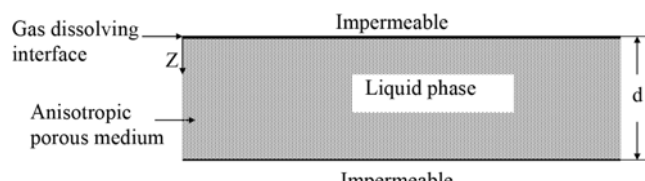


Fig. 1. Schematic diagram of system considered here.

[†]To whom correspondence should be addressed.

E-mail: mckim@cheju.ac.kr

centration C_i . The lower boundary is assumed to be impermeable and at no mass flux condition. The standard governing equations for the solute-driven convective mixing consist of Darcy's law for the fluid motion in a porous medium and the convective diffusion equation for the transport of the dissolved solute. Under the Boussinesq approximation, they can then be written as follows [1]:

$$\nabla \cdot \mathbf{U} = 0, \quad (1)$$

$$\frac{\mu}{K} \mathbf{U} = -\nabla P + \rho \beta g C, \quad (2)$$

$$\varepsilon \frac{\partial C}{\partial t} + \mathbf{U} \cdot \nabla C = \varepsilon \alpha_s \nabla^2 C, \quad (3)$$

where \mathbf{U} is the Darcy velocity vector, μ is the fluid viscosity, K is the absolute permeability tensor assumed constant everywhere but not necessarily isotropic, P is the pressure, \mathbf{g} is the gravitational acceleration, ε is the porosity C is the solute concentration, t is time, β is the volumetric expansion coefficient and α_s is the effective molecular diffusivity of the solute in the aqueous phase in the porous medium. The important parameters to describe the present system are the Darcy-Rayleigh number Ra_D and the anisotropic ratio γ defined by

$$Ra_D = \frac{g \beta d K_h C_i}{\varepsilon \alpha_s \nu} \text{ and } \gamma = \frac{K_v}{K_h},$$

where K_h and K_v denote the permeability in horizontal and vertical directions, respectively. The effect of an anisotropic permeability on the flow field was studied by Rees and Storesletten [20].

For the present transient stability analysis we define a set of nondimensionalized variables τ , z and c_0 by using the scale of time d^2/α_s , vertical length d and concentration C_i . Then the basic diffusion state is represented in dimensionless form by

$$\frac{\partial c_0}{\partial \tau} = \frac{\partial^2 c_0}{\partial z^2}, \quad (4)$$

with the following initial and boundary conditions:

$$c_0 = 0 \text{ at } \tau = 0, \quad (5a)$$

$$c_0 = 1 \text{ at } z = 0 \text{ and } \frac{\partial c_0}{\partial z} = 0 \text{ at } z = 1. \quad (5b)$$

The above equations can be solved by using conventional separation of variables technique or Laplace transform method as follows:

$$c_0 = 1 - 2 \sum_{n=0}^{\infty} \frac{\sin(\omega_n z)}{\omega_n} \exp(-\omega_n^2 \tau), \quad (6a)$$

$$c_0 = \sum_{n=0}^{\infty} (-1)^n \left\{ \operatorname{erfc}\left(\frac{n}{\sqrt{\tau}} + \frac{z}{2\sqrt{\tau}}\right) + \operatorname{erfc}\left(\frac{n+1}{\sqrt{\tau}} - \frac{z}{2\sqrt{\tau}}\right) \right\}, \quad (6b)$$

where $\omega_n = (n-1/2)\pi$. Eq. (6b) converges more rapidly than Eq. (6a) for a small time region. The evolution of the basic profiles of concentration with time is described in Fig. 2. For the deep-pool region of $\tau \leq 0.01$, the base concentration profiles reduced:

$$c_0 = \operatorname{erfc}\left(\frac{z}{2}\right), \quad (7)$$

where $\zeta = z/\sqrt{\tau}$. The above Leveque-type solutions of Eq. (7) are in good agreement with the exact solutions of Eq. (6) in the region

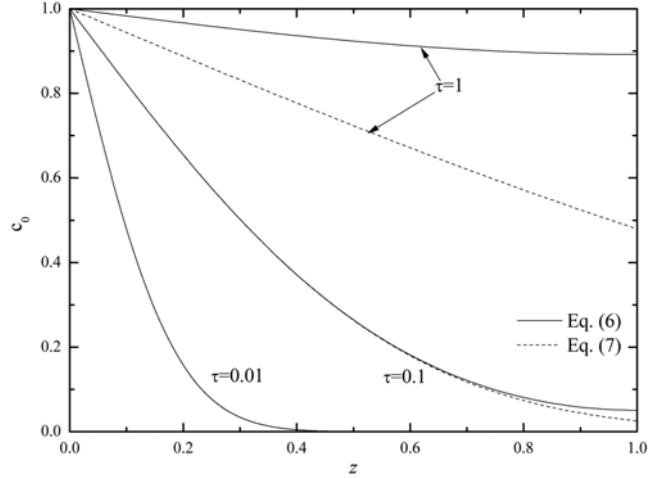


Fig. 2. The evolution of the basic profiles of concentration with time.

of $\tau < 0.1$. For $\tau \leq 0.01$ Eq. (6b) with $n=0$ yields almost the same concentration profile as Eq. (7).

2. Stability Equation

By perturbing Eqs. (1)-(3), we can obtain the following dimensionless equations:

$$\nabla' \cdot \mathbf{u}_1 = 0, \quad (8)$$

$$\mathbf{u}_1 + \nabla' p_1 - R c_1 \mathbf{k} = 0, \quad (9)$$

$$\frac{\partial c_1}{\partial \tau} = \nabla'^2 c_1 - R w_1 \frac{\partial c_0}{\partial z} - \mathbf{u}_1 \cdot \nabla' c_1 \quad (10)$$

under the following boundary conditions:

$$\mathbf{u}_1 = \mathbf{c}_1 = 0 \text{ at } z = 0, \quad (11a)$$

$$\mathbf{u}_1 = \frac{\partial c_1}{\partial z} = 0 \text{ at } z = 1, \quad (11b)$$

where $\nabla' = \mathbf{i} \sqrt{\gamma} \partial/\partial x + \mathbf{j} \sqrt{\gamma} \partial/\partial y + \mathbf{k} \partial/\partial z$ and \mathbf{i}, \mathbf{j} and \mathbf{k} are the unit vectors in the Cartesian coordinate and $R = \sqrt{Ra_D}$.

Now, multiplying Eq. (9) by \mathbf{u}_1 and Eq. (10) by c_1 , integrating them over the volume Ω and then employing the divergence theorem, Eqs. (9) and (10) become the following energy identities:

$$\frac{1}{2} \frac{\partial \langle |c_1|^2 \rangle}{\partial \tau} = -\langle |\nabla' c_1|^2 \rangle - R \left\langle w \frac{\partial c_0}{\partial z} c_1 \right\rangle, \quad (12)$$

$$0 = R \langle c_1 w_1 \rangle - \langle |\mathbf{u}_1|^2 \rangle, \quad (13)$$

where the primes have been dropped and $\langle \cdot \rangle = \int_{\Omega} (\cdot) d\Omega$. In the present system the dimensionless energy functional can be defined as a linear combination of Eqs. (12) and (13) with a coupling constant $\lambda > 0$:

$$E(\tau) = 0 + \frac{1}{2} \lambda \langle c_1 \rangle^2. \quad (14)$$

By setting $c_1 = \hat{c}_1 / \sqrt{\lambda}$, the above energy identity can be expressed as

$$\frac{dE}{d\tau} = -\langle |\nabla' c_1|^2 + |\mathbf{u}_1|^2 \rangle + R \left\langle \frac{w_1 c_1}{\sqrt{\lambda}} - \sqrt{\lambda} \frac{\partial c_0}{\partial z} w_1 c_1 \right\rangle, \quad (15)$$

where the hats have been dropped. The above relation can be repre-

sented as

$$\frac{dE}{dt} = RI - D \quad (16a)$$

where

$$I = \left\langle \frac{w_1 c_1}{\sqrt{\lambda}} - \sqrt{\lambda} \frac{\partial c_0}{\partial z} w_1 c_1 \right\rangle \quad (16b)$$

$$D = \langle |\nabla c_1|^2 + |\mathbf{u}_1|^2 \rangle \quad (16c)$$

The relative stability with respect to the most dangerous disturbances is guaranteed under the following condition [21]:

$$\sigma_i < \sigma_0 \text{ for all } \tau, \quad (17)$$

where $\sigma_i = (1/E)(dE/d\tau)$ and $\sigma_0 = (1/E_0)(dE_0/d\tau)$. Here E_0 is basic energy, i.e. $E_0 = \langle c_0^2 \rangle / 2$. The growth rate of disturbance energy σ_i is smaller than that of basic energy and the fluid layer is relatively stable when $R < R_\lambda$ where

$$\frac{1}{R_\lambda} = \max_\lambda \left(\frac{1}{\sigma_0 E + D} \right). \quad (18)$$

This maximum problem can be solved by the variational technique. In the usual manner the following Euler-Lagrange equations can be obtained:

$$\nabla' \cdot \mathbf{u}_i = 0, \quad (19)$$

$$\frac{1}{2} R_\lambda \left(\frac{1}{\sqrt{\lambda}} - \sqrt{\lambda} \frac{\partial c_0}{\partial z} \right) c_1 \mathbf{k} - \mathbf{u}_1 - \nabla' \phi = \mathbf{0}, \quad (20)$$

$$\nabla'^2 c_1 + \frac{\sigma_0}{2} c_1 + \frac{1}{2} R_\lambda \left(\frac{1}{\sqrt{\lambda}} - \sqrt{\lambda} \frac{\partial c_0}{\partial z} \right) w_1 = 0. \quad (21)$$

where ϕ is a Lagrangian multiplier.

Under the normal mode analysis, taking the double curl on Eq. (20), the following equations can be obtained.

$$\left(\frac{\partial^2}{\partial z^2} - a^2 \right) w_1 = -\frac{1}{2} R_\lambda \left(\frac{1}{\sqrt{\lambda}} - \sqrt{\lambda} \frac{\partial c_0}{\partial z} \right) \gamma a^2 c_1, \quad (22)$$

$$\left(\frac{\partial^2}{\partial z^2} - \gamma a^2 \right) c_1 = -\frac{\sigma_0}{2} c_1 - \frac{1}{2} R_\lambda \left(\frac{1}{\sqrt{\lambda}} - \sqrt{\lambda} \frac{\partial c_0}{\partial z} \right) w_1, \quad (23)$$

with the following boundary conditions

$$w_1 = c_1 = 0 \text{ at } z=0, \quad (24a)$$

$$w_1 = \frac{\partial c_1}{\partial z} = 0 \text{ at } z=1. \quad (24b)$$

The critical value Ra_D at which the growth rate of perturbation energy is less than that of basic energy for a whole range of time is given by

$$Ra_D^{1/2} = \max_\lambda \min_a R_\lambda \quad (25)$$

Based on the base concentration profile of Eq. (6a), σ_0 can be written as

$$\sigma_0 = \frac{\sum_{n=1}^{\infty} 4 \exp(-\omega_n^2 \tau) \{1 - \exp(-\omega_n^2 \tau)\}}{1 - \sum_{n=1}^{\infty} (2/\omega_n^2) \exp(-\omega_n^2 \tau) \{2 - \exp(-\omega_n^2 \tau)\}}. \quad (26)$$

For the limiting case of $\tau \rightarrow 0$, we can obtain $\sigma_0 = 1/2\tau$ from the concentration profile of Eq. (7), and rewrite the above stability equations by employing the similarity variable $\zeta = z/\sqrt{\tau}$ as,

$$(D^2 - a^*{}^2) w_1 = -\frac{1}{2} R_\lambda^* \left(\frac{1}{\sqrt{\lambda^*}} - \sqrt{\lambda^*} \frac{dc_0}{d\zeta} \right) \gamma a^*{}^2 c_1, \quad (27)$$

$$(D^2 - \gamma a^*{}^2) c_1 = -\frac{1}{4} c_1 - \frac{1}{2} R_\lambda^* \left(\frac{1}{\sqrt{\lambda^*}} - \sqrt{\lambda^*} Dc_0 \right) w_1, \quad (28)$$

with the following boundary conditions

$$w_1 = c_1 = 0 \text{ at } \zeta = 0, \quad (29a)$$

$$w_1 = Dc_1 = 0 \text{ as } \zeta \rightarrow \infty, \quad (29b)$$

where $D = d/d\zeta$, $R_\lambda^* = R_\lambda \tau^{1/4}$, and $a^* = a \tau^{1/2}$. For the isotropic case of $\gamma = 1$, the stability equations of Eqs. (27)-(29) are identical to those given by Kim and Choi [17] which were derived in (τ, ζ) -domain under the strong stability concept. And for another limiting case of $\tau \rightarrow \infty$, $\sigma_0 = 0$, which can be easily obtained from Eq. (26), and the above stability equations, Eqs. (22)-(25), degenerate into the strong stability formulation which was already analyzed by Hong and Kim [19]. Therefore, the present stability equations can cover the whole time region without any contradiction and assumption.

3. Solution Method

The stability Eqs. (22) and (23) are solved by employing the outward shooting scheme [22]. To integrate these stability equations the proper values of dw_1/dz and dc_1/dz at $z=0$ are assumed for a given τ , a , λ and γ . Since the stability equations and their boundary conditions are all homogeneous, the value of dw_1/dz at $z=0$ can be assigned arbitrarily and the value of the parameter R_λ is assumed. This procedure can be understood easily by taking into account the characteristics of eigenvalue problems. After all the values at $z=0$ are provided, this eigenvalue problem can proceed numerically. Integration is performed from $z=0$ to $z=1$ with the fourth-order Runge-Kutta-Gill method. If the guessed values of R_λ and dc_1/dz at $z=0$ are correct, w_1 and dc_1/dz will vanish at $z=1$. To improve the initial guesses the Newton-Raphson iteration is used.

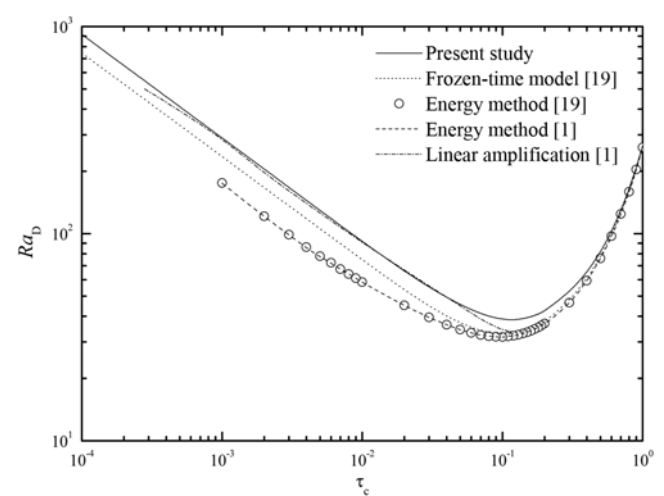


Fig. 3. Comparison of critical conditions for the isotropic case of $\gamma=1$.

RESULTS AND DISCUSSION

For the isotropic case of $\gamma=1$, the critical time τ_c from the various methods is compared in Fig. 3. Hong and Kim [19] extended the linear amplification theory up to the larger region of τ which Ennis-King et al. [1] and Hassanzadeh et al. [4] had never reached. Ennis-King et al. [1] and Hassanzadeh et al. [5] stopped their analyses near $\text{Ra}_{D,c}$ and therefore, τ_c is not able to be found in their linear amplification theory. For the large τ region of $\tau>0.1$, the frozen-time model, the energy method, the linear amplification theory and the present analysis give the nearly same results, and Ennis-King et al.'s [1] energy method supports our results. This proves our solution methods to be reasonable. As mentioned by Ennis-King et al. [1], for the region of small τ , the energy method is not capable of producing a critical condition due to the numerical accuracy. Even though Xu et al. [5] produced the critical condition for this region, their results are much lower than those of Ennis-King et al.'s [1] and the present work. Therefore, it seems that Xu et al.'s [5] results are numerically inaccurate. Hassanzadeh et al. [4] tried various types of initial conditions and found the most dangerous initial condition is the white noise condition.

For the region of $\tau<0.01$, where the effect of the lower boundary condition is insignificant, based on the linear amplification theory, Hassanzadeh et al. [4] suggested the lower bound of stability limit as $\tau_c=60\text{Ra}_D^{-2}$. Their lower bound is smaller than Ennis-King et al.'s [1] stability condition, $\tau_c=75\text{Ra}_D^{-2}$, even though the same initial condition was used in both studies. Hassanzadeh et al.'s [4] lower bound is quite close to our frozen-time model. This difference between the Hassanzadeh et al.'s [4] and Ennis-King et al.'s [1] may originate from the difference in the stability criteria. Ennis-King et al. [1] produced stability limits based on the following amplification factor of the averaged concentration disturbances:

$$\bar{c}=\left\{\int_0^1 c_1^2(\tau, z) dz / \int_0^1 c_1^2(0, z) dz\right\}^{1/2}, \quad (30)$$

whereas, Hassanzadeh et al. [4] used the following amplification factor of the averaged vertical velocity disturbances:

$$\bar{w}=\left\{\int_0^1 w_1^2(\tau, z) dz / \int_0^1 w_1^2(0, z) dz\right\}^{1/2}. \quad (31)$$

They traced the amplification of these quantities and chose the stability limits as $\partial\bar{c}/\partial\tau=0$ and $\partial\bar{w}/\partial\tau=0$. Recently, Rapaka et al. [6] defined the critical time $\tau_c^{(k)}$ as the time the most unstable disturbance reaches an amplification of 10^k , i.e., $\bar{c}=10^k$ at $\tau=\tau_c^{(k)}$. It is interesting that the present relaxed energy method predicts the nearly same critical time as that based on Ennis-King et al.'s [1] linear amplification theory.

Let's consider the effect of anisotropy on the critical conditions. For the mild anisotropic case of $\gamma=0.1$, the stability results are summarized in Fig. 4. The lower value of vertical permeability makes the system stable. For the large time of $\tau\geq 0.1$, Hong and Kim's critical times based on the energy method, and the frozen-time model and the present one are nearly the same. However, Hong and Kim's [19] energy method gives a quite different result from that of Ennis-King et al.'s [1]. For the region of $\tau\leq 0.1$, the present relaxed energy method gives the least conservative stability limit and Hong and

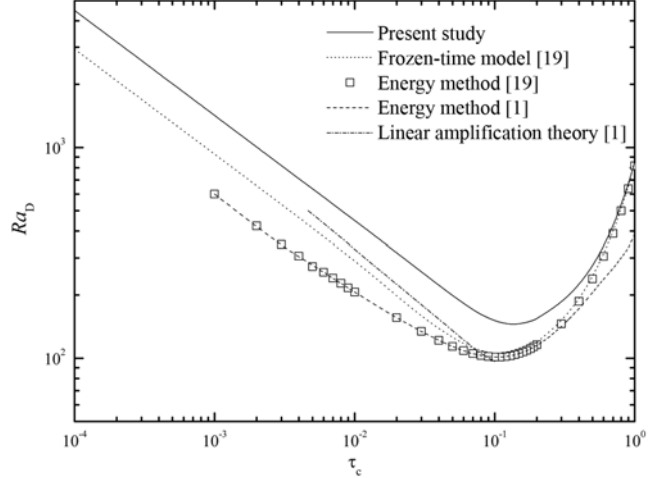


Fig. 4. Comparison of critical conditions for the moderate anisotropic case of $\gamma=0.1$.

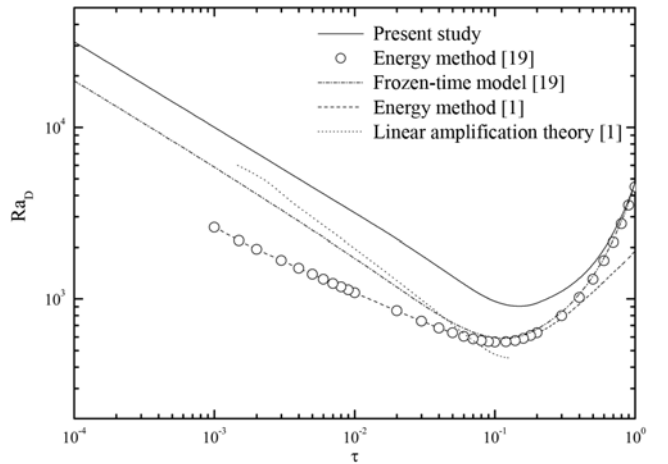


Fig. 5. Comparison of critical conditions for the strong anisotropic case of $\gamma=0.01$.

Kim's [18] stability characteristics reproduces Ennis-King et al.'s [1]. It is interesting that for the region of $\tau\geq 0.08$ the frozen-time model gives more stable results than the energy method. This reversal of tendency has never been observed in the isotropic case and even in other systems such as Rayleigh-Benard convections.

The stability results for the severe anisotropic case of $\gamma=0.01$ are summarized in Fig. 5. The much lower value of vertical permeability leads to a significant increase in Ra_D . This means that the strong anisotropic effect makes the system more stable and retards the CO_2 dissolution, as mentioned by Ennis-King and Paterson [2]. If other physical parameters such as thickness are fixed, this corresponds to a much later onset time for convection compared to the isotropic case. In Fig. 5, for the long time of $\tau\geq 0.5$ all methods predict almost the same results, while at $\tau\approx 0.1$, the stability characteristics are quite different from each other. For the long time of $\tau\geq 0.2$ the present results are quite different from that of Ennis-King et al.'s [1].

To obtain analytical scalings for the dependence of critical Rayleigh number for the onset of convection on the anisotropy ratio,

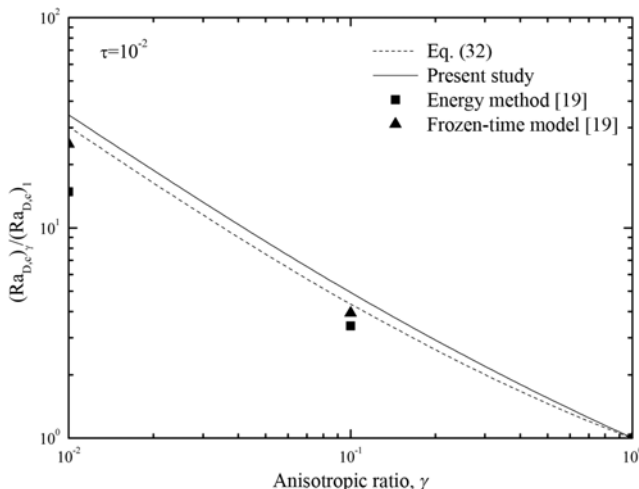


Fig. 6. Effect of anisotropy of porous media on the critical Darcy-Rayleigh number.

Ennis-King et al. [1] used single-term approximation and suggested the following relation:

$$\frac{(Ra_D^2 \tau_c)_\gamma}{(Ra_D^2 \tau_c)_1} = \frac{(1 + \sqrt{\gamma})^4}{16\gamma^2}. \quad (32)$$

In Fig. 6, the scaling proposed by Ennis-King et al. [1] and that obtained from the present work are compared. It can be seen that the present $Ra_{D,c}(\gamma)$ correspond closely with Eq. (32).

To validate the theoretical analysis, the predictions of τ_c should be compared with experimental observations. Recently, Ennis-King and Paterson [2] and Kneafsey and Pruess [23] conducted laboratory experiments for carbon dioxide-induced, density-driven convection in Hele-Shaw cells. However, they do not give all the data that is needed to calculate τ_c . To support and validate theoretical analyses, many researchers conducted various numerical simulations on the present problem [2-4,6]. Their stability analysis results are strongly dependent on the numerical scheme and the initial condition. Therefore, further studies are required to investigate the effect of initial conditions on the stability criterion.

It is well-known that convective mixing is the dominant mechanism for dissolution of CO_2 and the anisotropy effects retard the onset of buoyancy-driven convective motion. However, many other factors affect the onset condition, such as anisotropy of thermal or molecular diffusivity and temperature, concentration dependent viscosity variation and geothermal gradient. Therefore, many extensions of the present study including double diffusive convection are possible, and the variations of geological and physicochemical properties should be considered in real applications such as the dissolution of CO_2 into the stable aquifer.

CONCLUSIONS

The critical condition to mark the onset of convective motion in an initially quiescent, horizontal anisotropic porous layer has been analyzed by using the relaxed energy method. The resulting stability criteria compare reasonably well with previous theoretical predictions. And, the previous theoretical analyses are complemented

in the larger time domains and anisotropic cases. The anisotropy effect makes the system more stable and therefore decelerates the dissolution process. Various physical mechanisms related to dissolution, precipitation and geochemical reactions, which are not considered in the present analysis, can be expected to play a role in real dissolution process.

ACKNOWLEDGEMENT

This work was supported by the research grant from the Chuong-bong Academic Research Fund of Jeju National University in 2012.

NOMENCLATURE

a	: dimensionless wavenumber, $\sqrt{a_x^2 + a_y^2}$
C	: concentration [$kgmol/m^3$]
\bar{c}	: amplification factor of the averaged concentration disturbance
c_0	: dimensionless base concentration, C/C_i
c_1	: dimensionless concentration disturbance, $(g\beta C_1 K_h d)/(\varepsilon\alpha_s\nu)$
d	: porous layer depth [m]
g	: gravitational acceleration vector [m/s^2]
i, j, k	: unit vectors in the Cartesian coordinate
K	: permeability tensor [m^2]
P	: pressure [Pa]
p	: dimensionless pressure
Ra_D	: Darcy-Rayleigh number, $g\beta d K_h C_i / (\varepsilon\alpha_s\nu)$
t	: time [s]
U	: velocity vector [m/s]
u	: dimensionless velocity vector
\bar{w}	: amplification factor of the averaged vertical velocity disturbance
w_1	: dimensionless vertical velocity component
(x, y, z)	: dimensionless Cartesian coordinates

Greek Letters

α_s	: effective molecular diffusivity [m^2/s]
β	: densification coefficient [$m^3/kgmol$]
γ	: anisotropic ratio, K_v/K_h
λ	: coupling constant
μ	: viscosity [Pa·s]
ν	: kinematic viscosity [m^2/s]
ρ	: density [kg/m^3]
τ	: dimensionless time, $\alpha_s t/d^2$
ϕ	: Lagrangian multiplier

Subscripts

c	: critical states
0	: base quantities
1	: perturbed quantities

REFERENCES

1. J. Ennis-King, I. Preston and L. Paterson, *Phys. Fluids*, **17**, 084107 (2005).
2. J. Ennis-King and L. Paterson, *SPE J.*, 84344-PA (2005).
3. A. Riaz, M. Hesse, H. A. Tchelepi and F. M. Orr Jr., *J. Fluid Mech.*,

- 548**, 87 (2006).
4. H. Hassanzadeh, N. Pooladi-Darvish and D. Keith, *Trans. Porous Med.*, **65**, 193 (2006).
 5. X. Xu, S. Chen and Z. Zhang, *Adv. Water Res.*, **29**, 397 (2006).
 6. S. Rapaka, R. J. Pawar, P. H. Stauffer, D. Zhang and S. Chen, *J. Fluid Mech.*, **641**, 227 (2009).
 7. J. Hidalgo and J. Carrera, *J. Fluid Mech.*, **640**, 441 (2009).
 8. A. C. Slim and T. S. Ramakrishnan, *Phys. Fluids*, **22**, 124103 (2010).
 9. M. C. Kim and C. K. Choi, *Phys. Fluids*, **24**, 044102 (2012).
 10. M. T. Elenius, J. M. Nordbotten and H. Kalisch, *IMA J. Appl. Math.*, **77**, 771 (2012).
 11. C. W. Horton and F. T. Rogers, *J. Appl. Phys.*, **6**, 367 (1945).
 12. E. R. Lapwood, *Proc. Cambridge Phil. Soc.*, **44**, 508 (1948).
 13. J.-P. Caltagirone, *Q. J. Mech. Appl. Math.*, **33**, 47 (1980).
 14. D. Y. Yoon and C. K. Choi, *Korean J. Chem. Eng.*, **6**, 144 (1989).
 15. A. Selim and D. A. S. Rees, *J. Porous Media*, **10**, 1 (2007).
 16. H. Hassanzadeh, N. Pooladi-Darvish and D. W. Keith, *AICHE J.*, **53**, 1121 (2007).
 17. M. C. Kim and C. K. Choi, *Phys. Fluids*, **19**, 088103 (2007).
 18. D. A. Nield and A. Bejan, *Convection in Porous Media*, 4th Ed., Springer (2013).
 19. J. S. Hong and M. C. Kim, *Trans. Porous Media*, **72**, 241 (2008).
 20. D. A. S. Rees and L. Storesletten, *Trans. Porous Media*, **19**, 79 (1995).
 21. M. C. Kim, *Korean J. Chem. Eng.*, **30**, 831 (2013).
 22. M. C. Kim, *Korean J. Chem. Eng.*, **29**, 1688 (2012).
 23. T. J. Kneafsey and K. Pruess, *Transp. Porous Med.*, **82**, 123 (2010).